Nonuniform doping distribution along silicon nanowires measured by Kelvin probe force microscopy and scanning photocurrent microscopy

E. Koren, Y. Rosenwaks, J. E. Allen, E. R. Hemesath, and L. J. Lauhon

Citation: Appl. Phys. Lett. **95**, 092105 (2009); doi: 10.1063/1.3207887
View online: http://dx.doi.org/10.1063/1.3207887
View Table of Contents: http://apl.aip.org/resource/1/APPLAB/v95/i9
Published by the American Institute of Physics.

Nonuniform doping distribution along silicon nanowires measured by Kelvin probe force microscopy and scanning photocurrent microscopy

E. Koren,[1] Y. Rosenwaks,[1,a)] J. E. Allen,[2] E. R. Hemesath,[2] and L. J. Lauhon[2]
[1]*School of Electrical Engineering, Tel-Aviv University, Tel-Aviv 69978, Israel*
[2]*Department of Materials Science and Engineering, Northwestern University, 2220 Campus Drive, Evanston, Illinois 60208-3108, USA*

(Received 5 July 2009; accepted 27 July 2009; published online 1 September 2009)

We use Kelvin probe force microscopy and scanning photocurrent microscopy to measure the doping distribution along single phosphorous-doped silicon nanowire grown by the vapor-liquid-solid method. A nonlinear potential drop along biased silicon nanowires is detected both by measuring the surface potential directly via Kelvin probe force microscopy and by integrating the photocurrent measured by scanning photocurrent microscopy. These variations in the potential and field are further analyzed to extract the longitudinal dopant distribution along an individual silicon nanowire. The results show a very good agreement between the two methods to quantitatively detect potential, field, and doping variations within doped silicon nanowires. © *2009 American Institute of Physics*. [DOI: 10.1063/1.3207887]

Semiconductor nanowires are one of the most promising building blocks for near future nanoelectronics because they provide a route to continuing miniaturization as well as a wealth of opportunities in nanoscale science and technology.[1–4] There are many nanowire systems in which the majority carrier type is controlled by intentional doping, but in all cases the actual dopant concentration, its spatial distribution, and the fraction of active dopants are unknown.[5,6] Moreover, it has been recently reported that in silicon nanowires (SiNWs) grown by the widely used vapor–liquid-solid (VLS) growth method, there is a decreasing dopant concentration along the NWs toward the gold catalyst even when there is no indication of tapering.[7] This is a result of uncatalyzed incorporation of phosphorus atoms during growth. A nonuniform doping induces a nonlinear potential drop along NWs which conduct current. This profile has been extracted from scanning photocurrent microscopy (SPCM) measurements,[7] but correlation with direct potential measurements has not yet been reported. In this work we combine Kelvin probe force microscopy (KPFM) and SPCM to measure the variations in the active dopant concentration along *n*-SiNWs grown by the VLS method. Considering that KPFM measures the surface potential whereas SPCM samples the nanowire volume, the correlation between these two methods can improve our understanding regarding the role of surfaces in NWs electrical properties.

KPFM is by now a well-established method allowing a quantitative determination of surface potentials with nanometer spatial resolution. In principle, KPFM measures the contact potential difference (CPD) between a scanning tip and a sample.[8] A significant advantage of this technique is that it measures the potential by nullifying the tip-sample CPD; this ensures almost zero tip-induced band-bending which is very beneficial when measuring semiconducting materials.[9] It has been widely used to measure potential profiles of biased *p-n* junctions and organic semiconductor based field-effect transistors.[10] Recently it was also shown that defects in carbon nanotube devices could be identified using KPFM.[11] SPCM uses a focused laser spot to generate a local photocurrent that is extremely sensitive to the local electric field, enabling the extraction of the local electrostatic potential[7] or the minority carrier diffusion length.[12]

The *n*-type SiNWs used in this study were fabricated by low-pressure chemical vapor deposition with monodisperse 50 nm Au particles as catalysts for VLS growth. The growth was carried out at 460 °C and 40 torr with a source gas ratio of 1000:1 SiH_4 to PH_3, using N_2 as the carrier gas. Two-terminal devices on single NW were fabricated using electron-beam lithography and contact metallization with Ni [Fig. 1(a)]. Prior to metal evaporation, the contact area was exposed to oxygen plasma to remove residual resist and a 3 s wet etch with buffered HF solution to remove the native oxide. Two-terminal *I-V* characteristics were linear, confirming that the nanowires are the dominant resistance in the measured devices.[13] The KPFM measurements were conducted using a *Dimension 3100* atomic force microscopy (AFM) system in a controlled nitrogen environment glove box (less than ~5 ppm H_2O), in the lift mode where the first scan is a tapping mode topography measurement and in the second scan the tip is raised above the topography trajectory and measures the CPD. The SPCM measurements were performed using a *Witec* alpha300 confocal microscope to focus above-bandgap (532 nm) illumination onto a sample mounted on a piezoelectric scanning stage.

Since the KPFM measures the surface potential profile, it can be used as a "four-point-probe" where the scanning tip replaces the two inner contacts of the conventional setup. Although KPFM measures the potential at the surface, in the case of heavily doped wires used here, this potential can be considered, to a very good approximation, as the bulk NW potential. The current through the NW is measured and can be used to calculate the local effective doping, $N_D(x)$ along the SiNW. $j/E(x)=\sigma=q\mu N_D(x)$, where j is the current density, $E(x)$ is the local electric field, σ is the electrical conductivity, q is the elementary charge, and μ is the mobility for electrons. $E(x)$ is simply obtained by differentiating the measured surface potential along the NWs.

a)Electronic mail: yossir@eng.tau.ac.il.

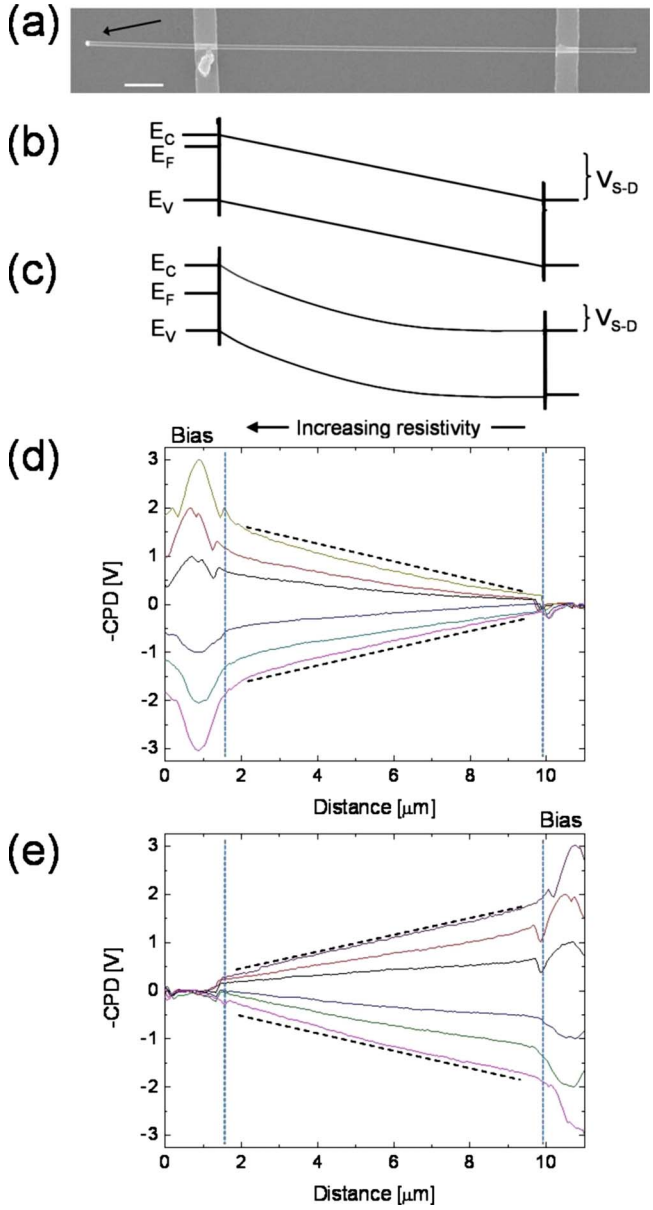

FIG. 1. (Color online) (a) HRSEM image of a typical NW device used in our measurements. The Au catalyst is marked by an arrow, contacts are made out of Ni, scale bar is 1 μm; schematic band-diagram for the case of a (b) uniform and (c) nonuniform doped SiNWs under an applied bias. (d) CPD measured profiles along *n*-SiNW biased at different voltages (-3 to 3 V with 1 V steps), applied to the gold catalyst end,(e) and to the other side. The perpendicular dotted lines (blue) represent the edges of the metal contacts. The dashed lines (black) are a guide to the eye to show the deviation from a linear potential profile in the case of a uniform doping distribution.

Figure 1(b) shows the expected potential profile along a biased SiNW for the case of uniform doping, in contrast to the case of gradually decreasing doping [Fig. 1(c)]. Figures 1(d) and 1(e) show the KPFM-measured surface potential profiles along an *n*-SiNW under several applied potentials (-3 to 3 V with 1 V steps). The voltage was applied by grounding one contact and biasing the other, while the back gate electrode was grounded throughout the whole measurement. The potential peaks are due to the applied bias at the left and the right metal contacts. The black dashed lines represent a linear potential drop and therefore help to visualize the deviation of the measured potential profiles from the case of a uniform doping concentration. The perpendicular dotted lines (blue) represent the edges of the metal contacts. When

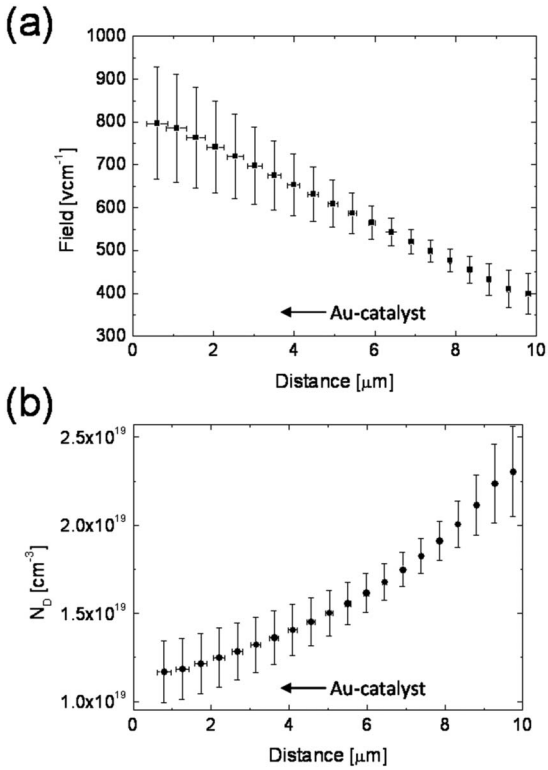

FIG. 2. (a) Averaged electric field and (b) doping profiles extracted from the measured KPFM profiles along biased *n*-SiNW (the average is between four cases where the applied bias was 1 and -1 V, each time for a different contact. The error bars represent the standard deviation of the four measurements).

applying the bias to the contact closer to the gold catalyst end, the surface potential profile is concave [Fig. 1(d)], while biasing the other contact the profile is convex [Fig. 1(e)]. Nevertheless, the absolute average electric field (the average was done for four measurements where the applied bias was 1 and -1 V, each time on a different contact; the error represents the standard deviation) is always larger near the gold catalyst [Fig. 2(a)], and therefore such a potential curvature is expected. For this reason, the observed field gradient is due to intrinsic variations within the NW itself rather than effects related to the metal electrodes. Furthermore, the field gradient is too small to cause significant variations in the local carrier mobility, so we assume a constant mobility of ~ 150 cm^2 V^{-1} s^{-1} (Ref. 14) throughout this paper consistent with electrons in bulk silicon doped to similar levels. This assumption, together with the measured potential, allows one to extract the longitudinal dopant distribution along the SiNW as explained above.

Figure 2(b) shows the averaged doping profile extracted by applying 1 and -1 V, each time for a different contact. The doping profile increases monotonically along the 8 μm long NW. The rate of increase is greater when the PH_3 partial pressure is increased.[7] In all cases, the doping is higher further from the catalyst side. This is consistent with the fact that this end of the wire was exposed a longer time to the PH_3 gas.

Next, we have used the potential profiles obtained by the SPCM for direct comparison to the KPFM data. Since the SPCM measurements were conducted on two-terminal devices, extraction of the absolute potential profiles from the SPCM-measured photocurrent required knowledge of a

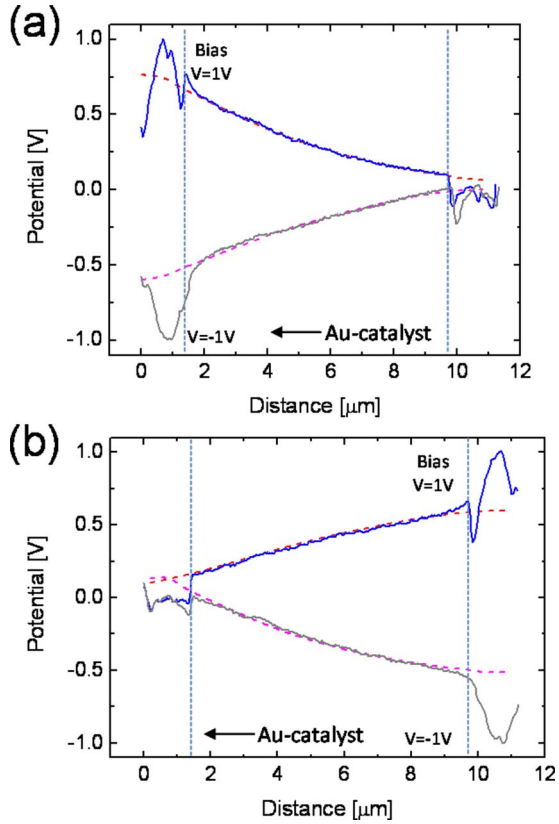

FIG. 3. (Color online) CPD (solid lines) and normalized integrated-photocurrent (dashed lines) profiles along biased *n*-SiNWs when the bias is applied to (a) the gold catalyst end and (b) to the other contact. The perpendicular dotted lines (blue) represent the edges of the metal contacts.

proportionality factor, representing the potential drop over the contacts, which can be determined by four-probe measurements.[7] Therefore, we have scaled and offset the integrated photocurrent profiles to fit the measured KPFM potential profiles, as the latter represent the actual NW potential. The scaling factor was 1.5 ± 0.1 for all curves. Figure 3 shows the normalized integrated-photocurrent profiles measured by the SPCM together with the KPFM measured potential profiles for the same wire under the same applied potentials (1 V, −1 V for each one of the contacts). The perpendicular dotted lines (blue) represent the edges of the metal contacts. Our results show an excellent agreement between these two methods, and confirm the validity of the potential measurements by the SPCM method.

There are several consequences of the observed nonuniform axial doping. As pointed out by others,[15,16] the synthesis of complex axial doping profiles is complicated by unintentional radial doping profiles. Surface doping may also diminish the influence of surface states on conductivity[17,18] by narrowing depletion layers. Even in the absence of surface states, a radially nonuniform doping profile will create a radially nonuniform potential and could produce carrier confinement at or away from the surface. Moreover, considering that KPFM measures the surface potential whereas SPCM the nanowire volume, the excellent agreement between the two methods and the fact that the surface is more heavily doped leads to the conclusion that most of the current flow takes place between the outer shell of the nanowire and its core.[19] Measurements of the radial doping profile are needed to understand how great the influence of this surface doping on operating devices is.

In summary, we have measured the variations in potential and electric field along biased *n*-Si nanowires by KPFM and SPCM, respectively. The potential profiles indicate a nonuniform doping along VLS based *n*-Si nanowires as recently reported.[7] This nonuniformity occurs as a result of the exposure of the NW surface to to PH_3 gas throughout the growth. In addition we have shown good correlation between KPFM and SPCM to quantitatively detect potential, field, and doping variations within doped Si nanowires.

This research was supported by Grant No. 2008140 from the United States–Israel Binational Science Foundation (BSF).

[1]Y. Cui and C. M. Lieber, Science **291**, 851 (2001).
[2]C. M. Lieber and Z. L. Wang, MRS Bull. **32**, 99 (2007).
[3]B. Z. Tian, X. L. Zheng, T. J. Kempa, Y. Fang, N. F. Yu, G. H. Yu, J. L. Huang, and C. M. Lieber, Nature (London) **449**, 885 (2007).
[4]M. S. Gudiksen, L. J. Lauhon, J. Wang, D. C. Smith, and C. M. Lieber, Nature (London) **415**, 617 (2002).
[5]Y. F. Wang, K. K. Lew, T. T. Ho, L. Pan, S. W. Novak, E. C. Dickey, J. M. Redwing, and T. S. Mayer, Nano Lett. **5**, 2139 (2005).
[6]C. Yang, Z. H. Zhong, and C. M. Lieber, Science **310**, 1304 (2005).
[7]J. E. Allen, D. E. Perea, E. R. Hemesath, and L. J. Lauhon, Adv. Mater. **21**, 3067 (2009).
[8]Y. Martin, D. W. Abraham, and H. K. Wickramasinghe, Appl. Phys. Lett. **52**, 1103 (1988).
[9]Y. Rosenwaks, R. Shikler, T. Glatzel, and S. Sadewasser, Phys. Rev. B **70**, 085320 (2004).
[10]V. Palermo, M. Palma, and P. Samori, Adv. Mater. **18**, 145 (2006).
[11]T. Umesaka, H. Ohnaka, Y. Ohno, S. Kishimoto, K. Maezawa, and T. Mizutani, Jpn. J. Appl. Phys., Part 1 **46**, 2496 (2007).
[12]Y. Gu, J. P. Romankiewicz, J. K. David, J. L. Lensch, and L. J. Lauhon, Nano Lett. **6**, 948 (2006).
[13]Z. Y. Zhang, K. Yao, Y. Liu, C. H. Jin, X. L. Liang, Q. Chen, and L. M. Peng, Adv. Funct. Mater. **17**, 2478 (2007).
[14]S. Banerjee and B. G. Streetman, *Solid State Electronic Devices*, 5th ed. (Prentice-Hall, Englewood Cliffs, 1999), p. 99.
[15]E. Tutuc, J. O. Chu, J. A. Ott, and S. Guha, Appl. Phys. Lett. **89**, 263101 (2006).
[16]T. J. Kempa, B. Tian, D. R. Kim, J. Hu, X. Zheng, and C. M. Lieber, Nano Lett. **8**, 3456 (2008).
[17]K. I. Seo, S. Sharma, A. A. Yasseri, D. R. Stewart, and T. I. Kamins, Electrochem. Solid-State Lett. **9**, G69 (2006).
[18]I. Kimukin, M. S. Islam, and R. S. Williams, Nanotechnology **17**, S240 (2006).
[19]E. Koren and Y. Rosenwaks (unpublished).